Interaction of Amino Acids with Gold and Silver Clusters

A. H. Pakiari* and Z. Jamshidi

Chemistry Department, College of Sciences, Shiraz University, Shiraz 71454, Iran

Received: January 14, 2007; In Final Form: March 12, 2007

Binding of gold and silver clusters with amino acids (glycine and cysteine) was studied using density functional theory (DFT). Geometries of neutral, anionic, and cationic amino acids with Au_3 and Ag_3 clusters were optimized using the DFT-B3LYP approach. The mixed basis set used here was denoted by 6-31+G** ∪LANL2DZ. This work demonstrated that the interaction of amino acids with gold and silver clusters is governed by two major bonding factors: (a) the anchoring N−Au(Ag), O−Au(Ag), and S−Au(Ag) bonds and (b) the nonconventional N−H···Au(Ag) and O−H···Au(Ag) hydrogen bonds. Among the three forms of amino acids, anionic ones exhibited the most tendency to interact with the Au and Ag clusters. Natural bond orbital analysis was performed to calculate charge transfer, natural population analysis, and Wiberg bond indices of the complexes. Atoms-in-molecules theory was also applied to determine the nature of interactions. It was shown that these bonds are partially electrostatic and partially covalent.

1. Introduction

Gold nanoparticles have attracted much attention in chemistry and material science because of their good biocompatibility, facile synthesis,[1] and conjugation to a variety of bimolecular ligands, antibodies, and other targeting moieties,[2] which make them suitable for the use in biochemical sensing and detection.[3−5] There have been several demonstrations of bioaffinity sensors based on the plasmon absorption and scattering of nanoparticle[3,4] and their assemblies,[5] so most experimental and theoretical investigations are focused on the interaction of gold with amino acids and DNA.[6]

Small clusters of coinage metals (Cu, Ag, and Au) have been studied by several experimental and theoretical works; the experimental studies concerning their chemical reactivity[7−10] were performed using resonant two-photon ionization,[11−13] photoelectron spectroscopy,[14−17] and Raman spectroscopy,[18] while many theoretical works have been devoted to the studies of the geometry, binding energy, and spectroscopic details of neutral,[19] anionic,[19d,20−22] and cationic clusters,[19f,20,23] especially for gold and silver.

Detection of amino acids is very important in proteomics. One of the major difficulties associated with the selective detection of α-amino acids and peptides using chemosensors is their structural similarity, incorporating both carboxylic and amino groups.[24] Among various amino acids, the S-containing cysteine and cystine amino acids are the most interesting because, being often on the border of large proteins, they provide a link to anchor proteins to metal compounds containing gold and silver. K. G. Thomas et al.[6k] have reported a novel strategy for the selective detection of micromolar concentrations of cysteine and glutathione by exploiting the interplasmon coupling in Au nanorods. They claimed that they can selectively detect micromolar concentration of cysteine/glutathione from a pool of α-amino acids. R. Di Felice et al.[6j] have studied the adsorption of the cysteine on the Au(111) surface, on the basis of DFT-PW91 calculations, and showed that the adsorption involves the S(thiolate)−Au bonds.

In this paper we have investigated theoretically the interaction of amino acids with Au_3 and Ag_3 clusters which serve as simple catalytic models of Au and Ag nanoparticles. The chosen amino acids are glycine and cysteine in three different forms (cationic (+), anionic (−), and neutral (∘)). Atoms-in-molecules (AIM) theory was applied to determine the nature of bonds between the amino acids and clusters. Natural bond orbital (NBO) analysis was also performed to calculate the charge transfer, Wiberg bond indices, and natural population analysis (NPA) of the complexes.

2. Method of Calculations

Geometries of the glycine and cysteine complexes, in their neutral, anionic, and cationic forms, with gold and silver trimmers (Au_3 and Ag_3) were fully optimized using the density functional theory (DFT) with B3LYP functional. The 6-31+G** basis set was used for the atoms in amino acids, while for gold and silver the Los Alamos effective-core potential (ECP) Lanl2DZ basis sets were applied.[25] In these basis sets, [Xe]4f inner electrons of Au and [Kr] inner electrons of Ag are treated as core electrons respectively, and their 11 outermost electrons are explicitly described using a double-ζ basis set.

The harmonic vibrational frequencies and corresponding zero-point vibrational energies (ZPVE) were calculated in all the optimized geometries, and real frequencies were obtained in all the cases. All the binding energies reported in this paper include the ZPVE correction.

In the present calculations the Gaussian 03 suite of programs was employed.[26] The NBO analysis[27] was conducted for these complexes in order to obtain the natural charges and Wiberg bond indices. The natural bond orbitals of several selected complexes were plotted using the GaussView program.[28] AIM analysis was performed with AIM2000 package[29] to calculate the properties of bond critical points (BCPs).

3. Results and Discussion

Trimmer clusters of gold and silver, Au_3 and Ag_3, were selected as simple catalytic models of Au and Ag nanoparticles,

* Corresponding author. E-mail address: pakiari@gmail.com.

10.1021/jp070306t CCC: $37.00
Published on Web 04/21/2007

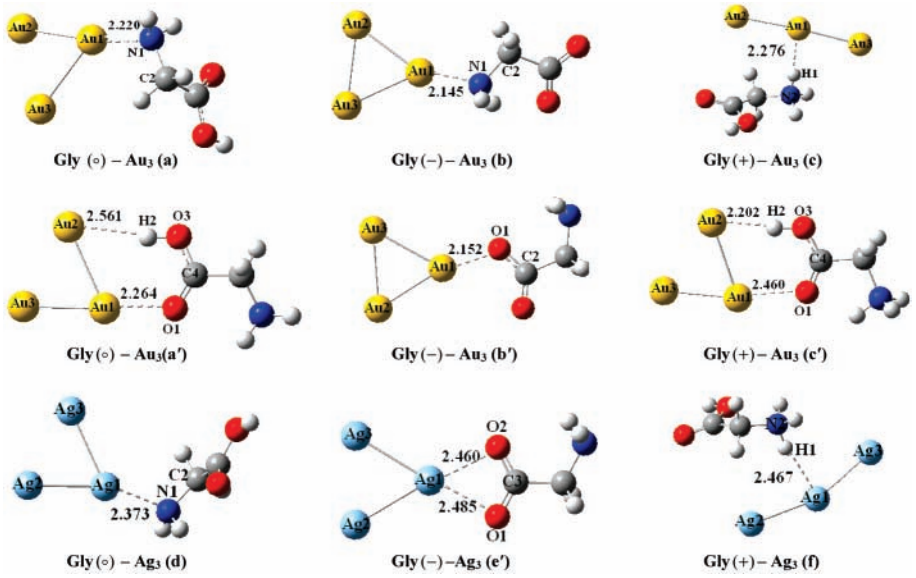

Figure 1. Optimized geometries of anionic, cationic, and neutral glycine with Au3 and Ag3 clusters; the bond lengths are given in angstroms.

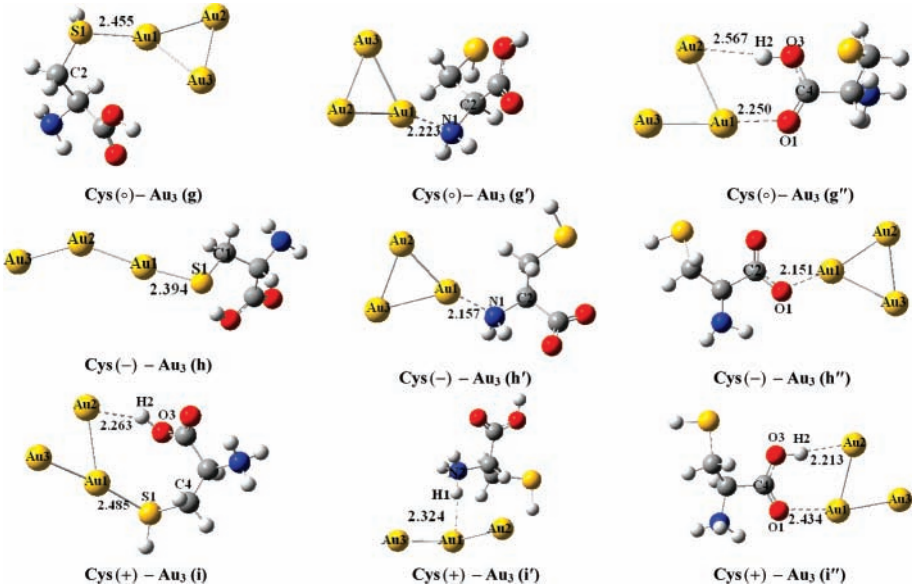

Figure 2. Optimized geometries of anionic, cationic, and neutral cysteine with Au3 cluster; the bond lengths are given in angstroms.

respectively. For the gold cluster, its equilibrium geometry was given by the bond lengths $r(Au_1-Au_2) = r(Au_2-Au_3) = 2.639$ Å and bond angle $\angle Au_1-Au_2-Au_3 = 140.91°$. These results are in good agreement with the results obtained from the DFT calculations[19f] using PW91PW91/LAL2DZ, PW91PW91/Stuttgart-1997, PW91PW91/CRENBL, and SVWN5/LANL2DZ as well as the spin-polarized DFT using plane wave basis sets.[19i] The calculated geometry has also been confirmed by the electron spin resonance (ESR) spectroscopy of the Au_3 cluster.[30]

For Ag_3, its equilibrium geometry has the bond lengths $r(Ag_1-Ag_2) = r\ (Ag_2-Ag_3) = 2.694$ Å and bond angle $\angle Ag_1-Ag_2-Ag_3 = 141.83°$. For neutral Au_3 and Ag_3 clusters the energy difference between the triangular and linear-like structures is very small. Lee et al.[19d] showed that DFT slightly favors the linear structure, while MP2 and CCSD slightly favor the triangular structure.

The initial geometries of glycine−Au_3(Ag_3) and cysteine−Au_3 complexes for optimization were generated by placing three gold and silver atoms near the active sites of glycine and cysteine. The active sites of these amino acids are amine, carboxylic, and sulfur groups. These groups have electron-rich nitrogen, oxygen, and sulfur that donate electron density to the 5d and 6s orbitals of Au and the 4d and 5s orbitals of Ag via their lone pairs. Gold and silver can also play the role as a proton acceptor and form nonconventional H-bonds with amine (N−H···Au(Ag)) and hydroxyl groups (O−H···Au(Ag)). The interaction between amino acids and metal clusters is either monodentate or bidentate, where in the latter case it usually involves non-conventional hydrogen bonding. The B3LYP/6-31+G** ∪LANL2DZ optimized structures of the neutral, anionic, and cationic forms of glycine and cysteine complexed to Au_3 and Ag_3 clusters are shown in Figures 1 and 2.

3.1. Structure and Energetics of Glycine−Au_3(Ag_3) Complexes. In the neutral glycine, Au_3 has a monodentate interaction through the amine group (Au−N) and bidentate interaction through the carboxylic group ((Au−O) and (Au···H−O)). As demonstrated in Table 1, for neutral Gly(o)−Au_3(a), the bond length r(Au−N) is equal to 2.220 Å, with a binding energy of 19.6 kcal mol^{-1}. It is clear from Table 1 that the C−N bond has been increased by 0.025 Å after the interaction with Au_3 cluster. In addition, the stretching mode of ν(C−N) undergoes a red shift with respect to that of the uncoordinated C−N group.

TABLE 1: Geometric Features of Anionic, Cationic, and Neutral Glycine with Au3 and Ag3 Clusters[a]

molecule	r(X−Au(Ag))	Δr(X−A)	$\Delta\nu$(X−A)	E_b
Gly(∘)−Au_3(a)	N_1−Au_1 (2.220)	N_1−C_2 (0.025)	N_1−C_2 (40.96)	−19.641
Gly(∘)−Au_3(a′)	H_2···Au_2 (2.561)	H_2−O_3 (0.021)	H_2−O_3 (415.55)	−11.985
	O_1−Au_1 (2.264)	O_1−C_4 (0.024)	O_1−C_4 (108.25)	
Gly(−)−Au_3(b)	N_1−Au_1 (2.145)	N_1−C_2 (0.016)	N_1−C_2 (97.6)	−44.113
Gly(−)−Au_3(b′)	O_1−Au_1 (2.152)	O_1−C_2 (0.032)	O_1−C_2 (317.89)	−43.925
Gly(+)−Au_3(c)	H_1···Au_1 (2.276)	H_1−N_2 (0.035)	H_1−N_2 (288.99)	−7.028
Gly(+)−Au_3(c′)	H_2···Au_2 (2.202)	H_2−O_3 (0.053)	H_2−O_3 (1054.88)	−7.781
	O_1−Au_1 (2.460)	O_1−C_4 (0.020)	O_1−C_4 (92.56)	
Gly(∘)−Ag_3(d)	N_1−Ag_1 (2.373)	N_1−C_2 (0.017)	N_1−C_2 (50.47)	−9.350
Gly(−)−Ag_3(e)	O_2−Ag_1 (2.460)	O_2−C_3 (0.003)	$O_{1,2-}$$C_3$ (44.05)	−33.006
	O_1−Ag_1 (2.485)	O_1−C_3 (0.005)		
Gly(+)−Ag_3(f)	H_1···Ag_1 (2.467)	H_1−N_2 (0.033)	H_1−N_2 (269.06)	−8.157

[a] r(X−Au(Ag)) is the length of the anchoring bond or nonconventional H-bonds, (X = O, N, S, and H). Δr(X−A) is the difference, in angstroms, between the bond lengths of N−C, O−C, N−H, and O−H in the complexed and isolated fragments. $\Delta\nu$(X−A), in cm^{-1}, is the difference between the frequency of N−C, O−C, N−H, and O−H bonds in the complexed and isolated fragments. The binding energy, E_b, includes zero-point vibrational energy and is in kcal mol^{-1}. The notations "(∘)", "(−)", and "(+)" indicate neutral, anionic, and cationic amino acids, respectively.

TABLE 2: Geometric Features of Anionic, Cationic, and Neutral Cysteine with Au3 Clusters[a]

molecule	r(X−Au)	Δr(X−A)	$\Delta\nu$(X−A)	E_b
Cys(∘)−Au_3(g)	S_1−Au_1 (2.455)	S_1−C_2 (0.017)	S_1−C_2 (54.92)	−14.997
Cys(∘)−Au_3(g′)	N_1−Au_1 (2.223)	N_1−C_2 (0.017)	N_1−C_2 (74.5)	−17.319
Cys(∘)−Au_3(g″)	O_1−Au_1 (2.250)	O_1−C_4 (0.025)	O_1−C_4 (109.29)	−10.228
	H_2···Au_2 (2.567)	H_2−O_3 (0.021)	H_2−O_3 (418.82)	
Cys(−)−Au_3(h)	S_1−Au_1 (2.394)	S_1−C_2 (−0.004)	S_1−C_2 (−41.52)	−58.357
Cys(−)−Au_3(h′)	N_1−Au_1 (2.157)	N_1−C_2 (0.027)	N_1−C_2 (37.43)	−38.968
Cys(−)−Au_3(h″)	O_1−Au_1 (2.151)	O_1−C_2 (0.034)	O_1−C_2 (66.18)	−38.905
Cys(+)−Au_3(i)	S_1−Au_1 (2.485)	S_1−C_4 (0.024)	S_1−C_4 (41.49)	−12.111
	H_2···Au_2 (2.263)	H_2−O_3 (0.041)	H_2−O_3 (819.73)	
Cys(+)−Au_3(i′)	H_1···Au_1 (2.324)	H_1−N_2 (0.036)	H_1−N_2 (385.33)	−7.906
Cys(+)−Au_3(i″)	O_1−Au_1 (2.434)	O_1−C_4 (0.019)	O_1−C_4 (91.52)	−5.522
	H_2···Au_2 (2.213)	H_2−O_3 (0.051)	H_2−O_3 (1018.87)	

[a] The parameters are defined in the footnote of Table 1.

Anionic glycine interacts with Au_3 through its NH_2 and COO^- groups and yields two strong anchoring bonds Au−N and Au−O with the corresponding bond lengths of 2.145 Å and 2.152 Å and bonding energies of 44.1 kcal mol^{-1} and 43.9 kcal mol^{-1}, respectively. Cationic glycine has a monodentate interaction through its NH_3 group and yields a nonconventional N−H···Au hydrogen bond with the bond length of 2.312 Å which is shorter than the van der Waals cutoff, r(H···Au) < $w_H + w_{Au}$ = 2.86 Å. The binding energy for this interaction equals 7.0 kcal mol^{-1}. Cationic glycine can also bind, in a bidentate way, to the Au_3 cluster with its carboxylic group through O and OH.

The geometry optimization was also performed for an anionic structure with a nonconventional H-bond as initial guess, but no minimum was finally found.

We averaged over all types of interaction the three forms glycine can have with Au_3. For example, neutral glycine interacts with Au_3 through the amine and carboxylic groups with the binding energies of 19.6 kcal mol^{-1} and 12.0 kcal mol^{-1}, respectively. So the averaged affinity of neutral glycine to Au_3 is thus 15.8 kcal mol^{-1}. The corresponding values for anionic and cationic glycine are 44.0 kcal mol^{-1} and 7.4 kcal mol^{-1}, respectively. Therefore, the anionic glycine possesses the highest affinity to gold cluster.

Silver cluster, Ag_3, behaves similarly to Au_3; however, its interaction with amino acids is weaker than the case of gold cluster. For example, the (Au−N) anchoring bond of neutral (Gly(o)−Au_3(a)) is 2.220 Å and its binding energy is 19.1 kcal mol^{-1}, while the corresponding bond in (Gly(∘)−Ag_3(d)) is 2.373 Å with the binding energy of 9.3 kcal mol^{-1}. E. S. Kryachko and F. Remacle[31] have suggested that two factors are mainly responsible for the weaker Ag bond: the lower polarizability of Ag_3 compared with Au_3, and the less extended 4d orbitals of Ag that are less involved in the electron density flow.

3.2. Structure and Energetic of the Cysteine−Au_3 Complex. Interaction of three forms of cysteine (neutral, anionic, and cationic) with the Au_3 cluster has been considered. Cysteine is able to anchor to gold through its amine, carboxylic, and sulfur groups to yield, respectively, (Au−N), (Au−O), (Au−S), (Au···H−O), and (N−H···Au) bonds. The calculated bond lengths, binding energies, and other parameters of these complexes are listed in Table 2. For anionic cysteine, the geometry optimization was also performed for a number of structures with nonconventional H-bond, and again no minimum was found.

The bond lengths and binding energies of (Au−N), (Au−O), (N−H···Au), and (Au···H−O) in different forms of cysteine do not differ much from the glycine counterparts. For example, the (Au···N) bond in Cys(∘)−Au_3(g′) is 2.223 Å and its binding energy is 17.3 kcal mol^{-1}, which are comparable to the values for the bond length and binding energy for the (Au−N) bond in Gly(∘)−Au_3(a) (bond length 2.220 Å and binding energy 19.6 kcal mol^{-1}). In all these cases the differences of the same anchoring bond lengths are less than 1% and binding energies less than 10%. In other words, the amino acid−metal cluster interaction through the amine and carboxylic groups remains the same for both glycine and cysteine. Therefore, the possibility of anchoring via the sulfur group becomes a characteristic to distinguish cysteine from glycine.

It is widely believed that the S−H bonds of thiol dissociates at the surface of gold and yields S(thiolate)−Au bonds.[32−33] In the anionic [Cys(−)−Au_3(h)], the S−H bond dissociates to form the S−Au bond, with the hydrogen atom absorbed by the COO^- group, while the S−H group retains in the neutral and

TABLE 3: Bond Critical Point Data (in a.u.) from AIM Analysis

molecule	BCP	ρ	$\nabla^2\rho$	$G(r)$	$V(r)$	$H(r)$
Gly(∘)−Au_3(a)	Au−N	0.080	0.320	0.093	−0.107	−0.014
Gly(∘)−Au_3(a′)	Au−O	0.062	0.292	0.078	−0.082	−0.004
Gly(−)−Au_3(b)	Au−N	0.094	0.369	0.111	−0.129	−0.018
Gly(−)−Au_3(b′)	Au−O	0.082	0.394	0.106	−0.113	−0.007
Gly(+)−Au_3(c)	Au···H	0.028	0.045	0.015	−0.019	−0.004
Gly(+)−Au_3(c′)	Au−O	0.041	0.168	0.045	−0.048	−0.003
	Au···H	0.034	0.039	0.016	−0.023	−0.007
Cys(∘)−Au_3(g)	Au−S	0.074	0.184	0.066	−0.086	−0.020
Cys(∘)−Au_3(g′)	Au−N	0.080	0.316	0.093	−0.106	−0.013
Cys(∘)−Au_3(g″)	Au−O	0.065	0.303	0.081	−0.085	−0.004
Cys(−)−Au_3(h)	Au−S	0.084	0.165	0.066	−0.092	−0.026
Cys(−)−Au_3(h′)	Au−N	0.093	0.353	0.107	−0.125	−0.018
Cys(−)−Au_3(h″)	Au−O	0.081	0.397	0.106	−0.114	−0.008
Cys(+)−Au_3(i)	Au−S	0.070	0.182	0.063	−0.081	−0.018
	Au···H	0.030	0.043	0.015	−0.020	−0.005
Cys(+)−Au_3(i′)	Au···H	0.029	0.045	0.016	−0.020	−0.004
Cys(+)−Au_3(i″)	Au−O	0.043	0.180	0.048	−0.051	−0.003
	Au···H	0.033	0.039	0.016	−0.022	−0.006

TABLE 4: Calculated NPA Charges and Wiberg Bond Indices of the Optimized Structures of Amino Acid−Metal Complexes

molecule	bond type	W_{Au-X}[a]	ΔW_{X-A}	ΔW_{Au-Au}	q_X	q_{Au}	$\Delta q_{cluster}$[b]
Gly(∘)−Au_3(a)	Au_1−N_1	0.235	−0.041	0.077	−0.954	0.239	−0.295
Gly(∘)−Au_3(a′)	Au_1−O_1	0.141	−0.179	0.065	−0.680	0.276	−0.031
	Au_2···H_2	0.060	−0.080		0.508	−0.219	
Gly(−)−Au_3(b)	Au_1−N_1	0.346	−0.052	0.099	−0.964	0.292	−0.253
Gly(−)−Au_3(b′)	Au_1−O_1	0.264	−0.184	0.097	−0.816	0.375	−0.207
Gly(+)−Au_3(c)	Au_1···H_1	0.129	−0.107	−0.001	0.437	−0.034	0.124
Gly(+)−Au_3(c′)	Au_1−O_1	0.066	−0.143	0.042	−0.675	0.176	0.127
	Au_2···H_2	0.169	−0.137		0.472	−0.138	
Cys(∘)−Au_3(g)	Au_1−S_1	0.329	−0.029	0.086	0.022	0.200	−0.186
Cys(∘)−Au_3(g′)	Au_1−N_1	0.234	−0.029	0.075	−0.950	0.231	−0.246
Cys(∘)−Au_3(g″)	Au_1−O_1	0.159	−0.198	0.063	−0.684	0.281	−0.060
	Au_2···H_2	0.053	−0.066		0.507	−0.214	
Cys(−)−Au_3(h)	Au_1−S_1	0.483	−0.005	−0.019	−0.370	0.134	−0.392
Cys(−)−Au_3(h′)	Au_1−N_1	0.332	−0.057	0.097	−0.958	0.284	−0.246
Cys(−)−Au_3(h″)	Au_1−O_1	0.254	−0.192	0.096	−0.817	0.377	−0.195
Cys(+)−Au_3(i)	Au_1−S_1	0.273	−0.030	0.092	0.054	0.146	−0.014
	Au_2···H_2	0.130	−0.113		0.494	−0.168	
Cys(+)−Au_3(i′)	Au_1···H_1	0.108	−0.093	0.102	0.414	−0.225	0.127
Cys(+)−Au_3(i″)	Au_1−O_1	0.070	−0.141	0.039	−0.681	0.187	0.119
	Au_2···H_2	0.164	−0.136		0.475	−0.142	

[a] X = N, O, S, and H. [b] $\Delta q_{cluster} = q_{Au3(complexed)} - q_{Au3(isolated)}$.

cationic counterparts. The bond lengths and binding energies of (Cys−Au_3) complexes are reported in Table 2.

The averaged affinities of cysteine to Au_3 are calculated and were found to be 14.2 kcal mol^{-1}, 45.4 kcal mol^{-1}, and 8.5 kcal mol^{-1} for neutral, anionic, and cationic cysteine, respectively. Again, the anionic one has the highest affinity to Au_3, as in the case of glycine.

3.3. Atoms-in-Molecules Analysis. In Bader's topological AIM analysis,[34] the nature of bonding interaction was analyzed in terms of the properties of electron density and its derivatives. We introduced some AIM parameters that are important in describing the bonding nature of the systems studied in Table 3.

Laplacian of $\rho(r)$ is related to the bond interaction energy by local expression of virial theorem.[35] A positive value of $\nabla^2\rho(r)$ shows a depletion of electronic charge along the bond. This is the case in a closed-shell electrostatic interaction. A negative value of $\nabla^2\rho(r)$, on the other hand, indicates that electronic charge is concentrated in the internuclear region. This is the case in an electron-sharing (or covalent) interaction.[35] A positive value of $\nabla^2\rho(r)$ at various BCPs of Au−X, in Table 3, indicates that these interactions are electrostatic in nature. The electronic energy density $H(r)$ at BCP is defined as $H(r) = G(r) + V(r)$, where $G(r)$ and $V(r)$ correspond to the kinetic and potential energy densities, respectively.[36] The sign of $H(r)$ determines whether the accumulation of charge at a given point r is stabilizing ($H(r) < 0$) or destabilizing ($H(r) > 0$). The calculated values of $H(r)$ reported in Table 3 are found to be negative, which implies a stabilizing effect due to the amassing charge in bond region and the presence of covalent bond. In Table 3, the calculated $H(r)$ values are negative for all Au−X bonds; these values become more negative for the same Au−X bond in anionic complex, indicating an increase in covalent character compared to the same bond of the neutral and cationic ones.

Therefore, from the positive value of $\nabla^2\rho(r)$ and negative value of $H(r)$, it has been concluded that Au−X bonds must be considered as partially covalent and partially electrostatic.[37]

It has been concluded, in section 3.2, that same Au−X bonds in glycine and cysteine do not differ much from each other. Using the computed AIM parameters, the same conclusions can be obtained. For instance, the AIM parameters calculated for the Au−N bond in the Gly(∘)−Au_3(a) complex ($\rho(r) = 0.080$, $\nabla^2\rho(r) = 0.320$, and $H(r) = -0.014$) are comparable to the values for the same bond in Cys(∘)−Au_3(g′) complex ($\rho(r) = 0.080$, $\nabla^2\rho(r) = 0.316$, and $H(r) = -0.013$).

3.4. Natural Population Analysis. Charge distributions of the active sites in the complexes are shown in Table 4. In many cases Au and X have opposite charges in the complex, which shows the electrostatic nature for the Au−X bond. (This result has been demonstrated by means of AIM analysis in section

TABLE 5: Results of Second-Order Perturbation Theory Analysis of the Fock Matrix within the NBO Basis for Some Selected Complexes

molecule	charge transfer	ΔE_{CT}	Δq_{CT}
Gly(∘)−Au_3(a)	$n_{N1} \rightarrow \sigma^*_{Au1-Au2}(\alpha)$	23.13	0.1053
	$n_{N1} \rightarrow n^*_{Au1}(\beta)$	27.09	0.1727
Gly(−)−Au_3(b)	$n_{O1} \rightarrow n^*_{Au1}(\alpha)$	32.02	0.2126
	$n_{O1} \rightarrow n^*_{Au1}(\beta)$	29.58	0.1964
Gly(+)−Au_3(c)	$n_{Au1} \rightarrow \sigma^*_{N2-H1}(\alpha)$	6.55	0.0222
	$n_{Au1} \rightarrow \sigma^*_{N2-H1}(\beta)$	3.91	0.0111
Cys(∘)−Au_3(g)	$n_{N1} \rightarrow \sigma^*_{Au1-Au2}(\alpha)$	21.45	0.095
	$n_{N1} \rightarrow n^*_{Au1}(\beta)$	25.60	0.157
Cys(−)−Au_3(h)	$n_{O1} \rightarrow n^*_{Au1}(\alpha)$	29.68	0.182
	$n_{O1} \rightarrow n^*_{Au1}(\beta)$	27.60	0.169
Cys(+)−Au_3(i)	$n_{Au1} \rightarrow \sigma^*_{N2-H1}(\alpha)$	14.00	0.043
	$n_{Au1} \rightarrow \sigma^*_{N2-H1}(\beta)$	3.63	0.013

3.3). Also it is evident that the differences of charges in gold cluster ($\Delta q_{cluster}$) are almost negative, suggesting that Au_3 cluster oxidizes the coordinated amino acid. The Wiberg bond indices[38] are helpful in evaluating the bond orders. The values of Wiberg bond indices for Au−X bonds are shown in Table 4. In agreement with the previous conclusion that the Au cluster tends to oxidize the amino acid, Wiberg bond indices for the same Au−X bonds have the order of anion > neutral > cation. For example, the Au−O bond index of Cys−Au_3 complex is 0.254 for anionic cysteine, and decreases to 0.070 for cationic cysteine. The differences of Wiberg bond indices between free and complexed amino acid (ΔW_{X-A}) are also shown in Table 4. In this table, all X−A (A = C in anchoring bonds and A = S, N, O in H-bonds) bond orders have been decreased after complexation, which shows that Au cluster has weakened the adjacent C−X bond in amino acid. It is worth noting that in almost all of the complexes, the Au cluster has reformed from its original shape (i.e., nearly linear in isolated state) to a triangular structure. This phenomenon can be explained by the existence of excess electrons in the Au cluster and is reflected by the increased Wiberg bond indices of terminal Au atoms ΔW_{Au-Au} which were shown in Table 4.

3.5. Natural Bond Orbital Analysis. NBOs provide the most accurate possible (natural Lewis structure) picture of the wavefunction ψ because all the orbital details are mathematically chosen so as to include the highest possible percentage of the electron density. A useful aspect of the NBO method is that it provides information about the interactions in both filled and virtual orbital spaces that facilitates the analysis of intra- and intermolecular interactions.

A second-order perturbation theory analysis of the Fock matrix was carried out to evaluate the donor−acceptor interaction in the NBO basis. The interactions result in a loss of occupancy from the localized NBOs of the idealized Lewis structure into the empty non-Lewis orbitals. For each donor NBO (i) and acceptor (j), the stabilization energy $E(2)$ associated with the delocalization $i \rightarrow j$ is estimated as

$$E(2) = \Delta E_{ij} = \Delta E_{CT} = -2\frac{\langle i|\hat{F}|j\rangle^2}{\epsilon_j - \epsilon_i}$$

where ϵ_i and ϵ_j are NBO orbital energies, and $\hat{F}$ is the Fock operator.

The quantities of transferred charge from a given donor orbital to a given acceptor orbital may be estimated again using the perturbation theory arguments, leading to the following approximate formula:

$$q_{CT} \approx 2\left(\frac{\langle i|\hat{F}|j\rangle}{\epsilon_j - \epsilon_i}\right)^2$$

In Table 5, ΔE_{CT} and Δq_{CT} for the anchoring Au−N, Au−O, and Au−S bonds of some complexes are listed. In these cases charge is transferred from the lone pair of nitrogen, oxygen, and sulfur to the σ^* and n* orbitals of Au. In the nonconventional N−H···Au and O−H···Au hydrogen bonds, charge is transferred from the lone pair of Au to the $\sigma^*_{N\rightarrow H}$ and $\sigma^*_{O\rightarrow H}$ orbitals. Figure 3 presents some typical NBOs responsible for the two charge-transfer processes between the metal cluster and amino acid. In Gly(∘)−Au_3(a), an electron is transferred from the lone pair of nitrogen to the σ^* and n* orbitals of gold. In Gly(+)−Au_3(c′), an electron is transferred from the lone pair of oxygen to the σ^* orbital of gold via the Au−O bond, while through the O−H···Au bond electron is transferred from the lone pair of gold to antibonding of O−H.

Charge-transfer interaction is associated with the shift of occupancy from the manifold of filled orbitals of one monomer to the unfilled orbitals of the other. Therefore, ΔE_{CT} can be estimated by deleting the Fock matrix elements connecting these manifolds and calculating the change in the total energy. We estimated ΔE_{del} to be 36.51 kcal mol^{-1} for Gly(∘)−Au_3(a′) complex by deleting the off-diagonal elements of the Fock matrix responsible for the charge transfer. This value is close to the computed ΔE_{CT} of 43.11 kcal mol^{-1}.

Not only does the charge transfer result in an increase in the binding energy but it also allows a significant overcoming of the exclusion repulsion, thus permitting the molecules to approach each other beyond the van der Waals contact distance. To test this effect, the geometry of the Gly(∘)−Au_3(a′) complex

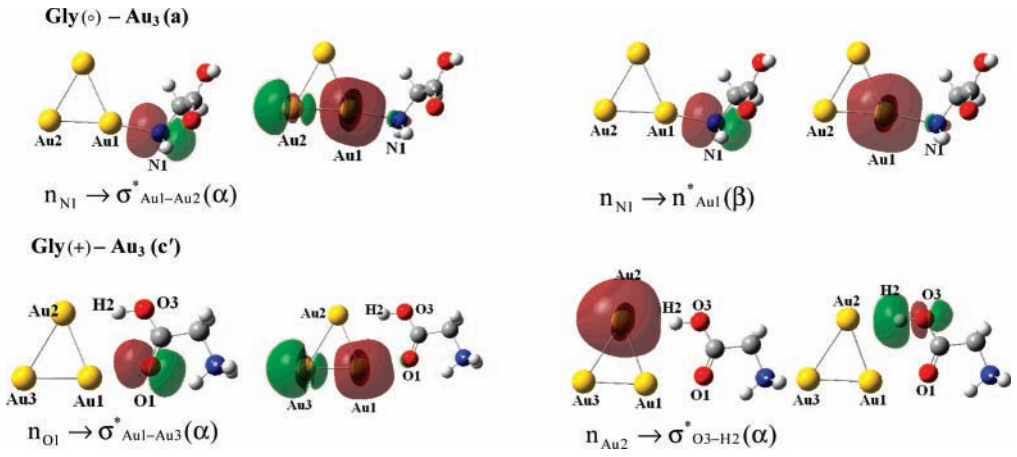

Figure 3. NBO orbitals associated with charge-transfer analysis.

was reoptimized at the B3LYP/6-31+G** ∪LANL2DZ level with the deleted charge-transfer effects. The O_1-Au_1 bond length was found to stretch by 0.790 Å, and the $H_2\cdots Au_2$ bond elongates by 1.088 Å.

4. Conclusions

Interaction of two selected amino acids (glycine and cysteine) with gold and silver clusters have been described in the geometrical, spectroscopic, and energetic aspects. Two major bonding factors were found to govern the interaction of these metals with amino acids: the anchoring bonds (N−Au(Ag), O−Au(Ag), and S−Au(Ag)) and the nonconventional (N−H···Au(Ag) and O−H···Au(Ag)) hydrogen bonds. These bonds have been observed in the complexes involving neutral, cationic, and anionic amino acids. The anionic amino acids have the highest averaged affinities to the metal clusters. The interactions of metal clusters to amino acids through the amine and carboxylic groups are almost the same for the two types of amino acids, so we can conclude that the metal−sulfur bond to these clusters could help distinguish cysteine from the other amino acids.

The bond lengths of X−A in amino acid increase after complexation, and the stretching modes of these bonds undergo a red shift with respect to isolated ones. Ag cluster shows similar behavior to Au cluster, but its bonding to amino acids is weaker.

AIM analysis was performed to extract the bond critical point properties. It was found that $\nabla^2\rho(r)$ and $H(r)$ for the anchoring bonds are respectively positive and negative, revealing that these bonds are partially electrostatic and partially covalent.

The results from NPA suggests that the Au_3 cluster tends to oxide the coordinated amino acids, and the Wiberg bond indices show the bond order of anion > neutral > cation for the same Au−X bond in the complexes.

Second-order perturbation analysis was used to show the effect of charge transfer in the formation of these complexes. For the anchoring bonds, lone pair electrons of sulfur, oxygen, and nitrogen are transferred to the antibonding orbitals of the metal, while for the nonconventional hydrogen bonds, the lone pair electrons of metal are transferred to the antibonding orbitals of N−H and O−H bonds.

References and Notes

(1) Burda, C.; Chen, X.; Narayanan, R.; El-Sayed, M. A. *Chem. Rev.* **2005**, *105*, 1025.

(2) Katz, E.; Willner, I. *Agnew. Chem., Int. Ed.* **2004**, *43*, 6042.

(3) Riboh, J. C.; Haes, A. J.; McFarland, A. D.; Ranjit, C.; Van Duyne, R. P. *J. Phys. Chem. B* **2003**, *107*, 1772.

(4) Shafer-Peltier, K. E.; Haynes, C. L.; Glucksberg, M. R.; Van Duyne, R. P. *J. Am. Chem. Soc.* **2003**, *125*, 588.

(5) Storhoff, J. J.; Elghanian, R.; Mucic, R. C.; Mirkin, C. A.; Letsinger, R. L. *J. Am. Chem. Soc.* **1998**, *120*, 1959.

(6) (a) Kryachko, E. S.; Remacle, F. *Nano Lett.* **2005**, *5*, 735. (b) Kumar, A.; Mishra, P. C.; Suhai, S. *J. Phys. Chem. A* **2006**, *110*, 7719. (c) Kryachko, E. S.; Remacle, F. *J. Phys. Chem. B* **2005**, *109*, 22746. (d) Thaxton, C. S.; Georganopoulou, D. G.; Mirkin, C. A. *Clin. Chim. Acta.* **2006**, *363*, 120. (e) Kühnle, A.; Linderoth, T. R.; Hammer, B.; Besenbacher, F. *Nature* **2002**, *415*, 891. (f) Wang, J. *Anal. Chim. Acta.* **2003**, *500*, 247. (g) Zhong, Z.; Patskovskyy, S.; Bouvrette, P.; Luong, J. H. T.; Gedanken, A. *J. Phys. Chem. B* **2004**, *108*, 4046. (h) Garzón, I. L.; Artacho, E.; Beltrán, M. R.; García, A.; Junquera, J.; Michaelian, K.; Ordejón, P.; Rovira, C.; Sánchez-Portal, D.; Soler, J. M. *Nanotechnology* **2001**, *12*, 126. (i) Huang, Y. F.; Lin, Y. W.; Chang, H. T. *Nanotechnology* **2006**, *17*, 4885. (j) Felice, R. D.; Selloni, A.; Molinari, E. *J. Phys. Chem. B* **2003**, *107*, 1151. (k) Sudeep, P. K.; Joseph, S. T. S.; Thomas, K. G. *J. Am. Chem. Soc.* **2005**, *127*, 6516. (l) Slocik, J. M.; Moore, J. T.; Wright, D. W. *Nano Lett.* **2002**, *2*, 169, 1151.

(7) Lee, T. H.; Ervin, K. M. *J. Phys. Chem.* **1994**, *98*, 10023.

(8) Bucher, S. W.; Gold, J. R.; Freiser, B. S. *J. Chem. Phys.* **1988**, *88*, 3678.

(9) Cheeseman, M. A.; Eyler, J. R. *J. Phys. Chem.* **1992**, *96*, 1082.

(10) Lian, L.; Hackett, P. A.; Rayner, D. M. *J. Chem. Phys.* **1993**, *99*, 2583.

(11) Bishea, G. A.; Arrington, C. A.; Behm, J. M.; Morse, M. D. *J. Chem. Phys.* **1991**, *95*, 8765.

(12) Bishea, G. A.; Pinegar, J. C.; Morse, M. D. *J. Chem. Phys.* **1991**, *95*, 5630.

(13) Pinegar, J. C.; Langenberg, J. D.; Morse, M. D. *Chem. Phys. Lett.* **1993**, *212*, 458.

(14) Taylor, K. J.; Pettiette-Hall, C. L.; Cheshnovsky, O.; Smally, R. E. *J. Chem. Phys.* **1992**, *96*, 3319.

(15) Ho, J.; Ervin, K. M.; Lineberger, W. C. *J. Chem. Phys.* **1990**, *93*, 6987.

(16) Handshuh, H.; Cha, C. Y.; Bechthold, P. S.; Ganteför, G.; Eberhart, W. *J. Chem. Phys.* **1995**, *102*, 6406.

(17) Handshuh, H.; Bechthold, P. S.; Ganteför, G.; Eberhart, W. *J. Chem. Phys.* **1994**, *100*, 7093.

(18) Haslett, T. L.; Bosnick, K. A.; Moskovits, M. *J. Chem. Phys.* **1998**, *108*, 3453.

(19) (a) Balasubramanian, K.; Liao, D. *J. Chem. Phys.* **1991**, *94*, 5233. (b) Balasubramanian, K.; Liao, D. *J. Chem. Phys.* **1992**, *97*, 2548. (c) Zheng, J.; Petty, J. T.; Dickson, R. M.; *J. Am. Chem. Soc.* **2003**, *125*, 7780. (d) Lee, H. M.; Ge, M.; Sahu, B. R.; Tarakeshwar, P.; Kim, K. S. *J. Phys. Chem. B* **2003**, *107*, 9994. (e) Soule de Bas, B.; Ford, M. J.; Cortie, M. B. *J. Mol. Struct.: THEOCHEM* **2004**, *686*, 193. (f) Walker, A. V. *J. Chem. Phys.* **2005**, *122*, 094310. (g) Yuan, D. W.; Wang, Y.; Zeng, Z. *J. Chem. Phys.* **2005**, *122*, 114310. (h) Xiao, L.; Wang, L. *Chem. Phys. Lett.* **2004**, *392*, 452. (i) Xiao, L.; Tollberg, B.; Hu, X.; Wang, L. *J. Chem. Phys.* **2006**, *124*, 114309.

(20) Remacle, F.; Kryachko, E. S. *J. Chem. Phys.* **2005**, *122*, 044304.

(21) Agrawal, B. K.; Agrawal, S.; Srivastava, P.; Singh, S. *J. Nanoparticle. Res.* **2004**, *6*, 363.

(22) (a) Furche, F.; Ahlrichs, R.; Weis, P.; Jacob, C.; Gilb, S.; Bierweiler, T.; Kappes, M. M. *J. Chem. Phys.* **2002**, *117*, 6982. (b) Hakkinen, H.; Moseler, M.; Landman, U. *Phys. Rev. Lett.* **2002**, *89*, 033401. (c) Kim, Y. D.; Fischer, M.; Gantefor, G. *Chem. Phys. Lett.* **2003**, *377*, 170. (d) Niemietz, M.; Gerhardt, P.; Gantefor, G.; Kim, Y. D. *Chem. Phys. Lett.* **2003**, *380*, 99.

(23) (a) Gilb, S.; Weis, P.; Furche, F.; Ahlrichs, R.; Kappes, M. M. *J. Chem. Phys.* **2002**, *116*, 4094. (b) Weis, P.; Welz, O.; Vollmer, E.; Kappes, M. M. *J. Chem. Phys.* **2004**, *120*, 677. (c) Fielicke, A.; von Helden, G.; Meijer, G.; Pedersen, D. B.; Simard, B.; Rayner, D. M. *J. Am. Chem. Soc.* **2005**, *127*, 8416.

(24) Ait-Haddou, H.; Wiskur, S. L.; Lynch, V. M.; Anslyn, E. V. *J. Am. Chem. Soc.* **2001**, *123*, 11296.

(25) (a) Hay, P. J.; Wadt, W. R. *J. Chem. Phys. Chem.* **1985**, *82*, 270. (b) Hay, P. J.; Wadt, W. R. *J. Chem. Phys. Chem.* **1985**, *82*, 284. (c) Hay, P. J.; Wadt, W. R. *J. Chem. Phys. Chem.* **1985**, *82*, 299.

(26) Frisch, M. J.; Trucks, G. W.; Schlegel, H. B.; Scuseria, G. E.; Robb, M. A.; Cheeseman, J. R.; Montgomery, J. A., Jr.; Vreven, T.; Kudin, K. N.; Burant, J. C.; Millam, J. M.; Iyengar, S. S.; Tomasi, J.; Barone, V.; Mennucci, B.; Cossi, M.; Scalmani, G.; Rega, N.; Petersson, G. A.; Nakatsuji, H.; Hada, M.; Ehara, M.; Toyota, K.; Fukuda, R.; Hasegawa, J.; Ishida, M.; Nakajima, T.; Honda, Y.; Kitao, O.; Nakai, H.; Klene, M.; Li, X.; Knox, J. E.; Hratchian, H. P.; Cross, J. B.; Adamo, C.; Jaramillo, J.; Gomperts, R.; Stratmann, R. E.; Yazyev, O.; Austin, A. J.; Cammi, R.; Pomelli, C.; Ochterski, J. W.; Ayala, P. Y.; Morokuma, K.; Voth, G. A.; Salvador, P.; Dannenberg, J. J.; Zakrzewski, V. G.; Dapprich, S.; Daniels, A. D.; Strain, M. C.; Farkas, O.; Malick, D. K.; Rabuck, A. D.; Raghavachari, K.; Foresman, J. B.; Ortiz, J. V.; Cui, Q.; Baboul, A. G.; Clifford, S.; Cioslowski, J.; Stefanov, B. B.; Liu, G.; Liashenko, A.; Piskorz, P.; Komaromi, I.; Martin, R. L.; Fox, D. J.; Keith, T.; Al-Laham, M. A.; Peng, C. Y.; Nanayakkara, A.; Challacombe, M.; Gill, P. M. W.; Johnson, B.; Chen, W.; Wong, M. V.; Gonzalez, C.; Pople, J. A. *Gaussian 03*, Revision B.04; Gaussian, Inc.: Pittsburgh, PA, 2003.

(27) Reed, A. E.; Curtiss, L. A.; Weinhold, F. *Chem. Rev.* **1988**, *88*, 899.

(28) *GaussView*; Gaussian, Inc.: Pittsburgh, PA, 2003.

(29) Bader, R. F. W. *AIM2000 Program Package*, Ver. 2.0; McMaster University: Hamilton, Ontario, Canada, 2002.

(30) Howard, J. A.; Sutcliffe, R.; Mile, B. *J. Chem. Soc. Chem. Commun.* **1983**, 1449.

(31) Kryachko, E. S.; Remacle, F. *Chem. Phys. Lett.* **2005**, *404*, 142.

(32) Poirier, G. E. *Chem. Rev.* **1997**, *97*, 1117.

(33) Grönbeck, H.; Curioni, A.; Andreoni, W. *J. Am. Chem. Soc.* **2000**, *122*, 2839.

(34) Bader, R. F. W. *Chem. Rev.* **1991**, *91*, 893.

(35) Bader, R. F. W. *Atoms in molecules: a quantum theory*; Oxford University Press: Oxford, U.K., 1990.

(36) Cremer, D.; Kraka, E. *Angew. Chem.* **1984**, *23*, 627.

(37) Bianchi, R.; Gervasio, G.; Marabello, D. *Inorg. Chem.* **2000**, *39*, 2360.

(38) Wiberg, K. *Tetrahedron* **1968**, *24*, 1093.